Heliyon 8 (2022) e09878

Contents lists available at ScienceDirect

Heliyon

journal homepage: www.cell.com/heliyon

Research article

Integrated analysis of the clinical consequence and associated gene expression of *ALK* in *ALK*-positive human cancers

Saifullah [a,b], Toshifumi Tsukahara [a,c,*]

[a] *Area of Bioscience and Biotechnology, School of Materials Science, Japan Advanced Institute of Science and Technology (JAIST), 1–1 Asahidai, Nomi City, Ishikawa, 923-1292, Japan*
[b] *Department of Molecular Therapy, National Institute of Neuroscience, National Center of Neurology and Psychiatry (NCNP), Kodaira City, Tokyo, 187-8502, Japan*
[c] *Division of Transdisciplinary Science, Japan Advanced Institute of Science and Technology (JAIST), 1–1 Asahidai, Nomi City, Ishikawa, 923-1292, Japan*

ARTICLE INFO

Keywords:
ALK expression
Patient prognosis
LUAD
Co-expression
Cancers

ABSTRACT

Anaplastic lymphoma kinase (ALK) is a tyrosine kinase receptor that is genetically altered in several cancers, including NSCLC, melanoma, lymphoma, and other tumors. Although *ALK* is associated with various cancers, the relationship between *ALK* expression and patient prognosis in different cancers is poorly understood. Here, using multidimensional approaches, we revealed the correlation between *ALK* expression and the clinical outcomes of patients with LUAD, melanoma, OV, DLBC, AML, and BC. We analyzed *ALK* transcriptional expression, patient survival rate, genetic alteration, protein network, and gene and microRNA (miRNA) co-expression. Compared to that in normal tissues, higher *ALK* expression was found in LUAD, melanoma, and OV, which are associated with poor patient survival rates. In contrast, lower transcriptional expression was found to decrease the survival rate of patients with DLBC, AML, and BC. A total of 202 missense mutations, 17 truncating mutations, 7 fusions, and 3 in-frame mutations were identified. Further, 17 genes and 19 miRNAs were found to be exclusively co-expressed and echinoderm microtubule-associated protein-like 4 (*EML4*) was identified as the most positively correlated gene (log odds ratio >3). The gene ontology and signaling pathways of the genes co-expressed with *ALK* in these six cancers were also identified. Our findings offer a basis for *ALK* as a prognostic biomarker and therapeutic target in cancers, which will potentially contribute to precision oncology and assist clinicians in identifying suitable treatment options.

1. Introduction

Anaplastic lymphoma kinase (ALK) is a transmembrane tyrosine kinase receptor belonging to the insulin receptor superfamily [1]. Genetic aberrations of *ALK*, including gene fusions, translocations, or inversions with different gene partners, have been identified in different cancers, such as *EML4-ALK* oncofusion in non-small cell lung cancer (NSCLC) [2, 3], nucleophosmin (*NPM*)-*ALK* fusion oncogene in anaplastic large cell lymphoma (ALCL) [4], truncating *ALK* in melanoma [5], and translocation of *ALK* in ovarian serous carcinoma [6]. *ALK* translocations also appear at low rates in diffuse large B-cell lymphoma (DLBC) [7], acute myeloid leukemia (AML) [8], breast cancer (BC) [9], and renal cell carcinomas [10]. The resultant ALK chimeraproteins comprise the C-terminal part of the entire intracellular tyrosine kinase domain and the N-terminal part of the fusion proteins, usually the di- or trimerization domain [11].

Once the fusion protein is activated by di- or trimerization, ALK plays a primary role in constitutive autophosphorylation, leading to the activation of downstream signaling and subsequent arrest of cell proliferation and growth. There are four main signaling pathways downstream of kinase-activated ALK: proto-oncogene protein p21/extracellular-signal-regulated kinase (RAS/ERK), phosphoinositol-3 kinase (PI3K)/Akt, Janus kinase/signal transducer and activator of transcription (JAK/STAT), and phospholipase Cγ (PLCγ) [12]. ALK also activates adapter and cellular proteins, including Src, IRS2, PTPN11, FAK, Shc-GRB2, GSK-3a, and FRS2, suggesting signaling as alternative pathways [13]. Furthermore, *ALK* is oncogenically activated by overexpression [14], point mutation [15], or truncation [16]. These discrete cellular functions and activation of downstream cascades contribute to the initiation and development of multiple malignancies.

Multi-omics data and clinical information have revolutionized the field of medicine and biology, enabling a comprehensive understanding

* Corresponding author.
E-mail address: tukahara@jaist.ac.jp (T. Tsukahara).

https://doi.org/10.1016/j.heliyon.2022.e09878
Received 28 September 2021; Received in revised form 30 January 2022; Accepted 1 July 2022

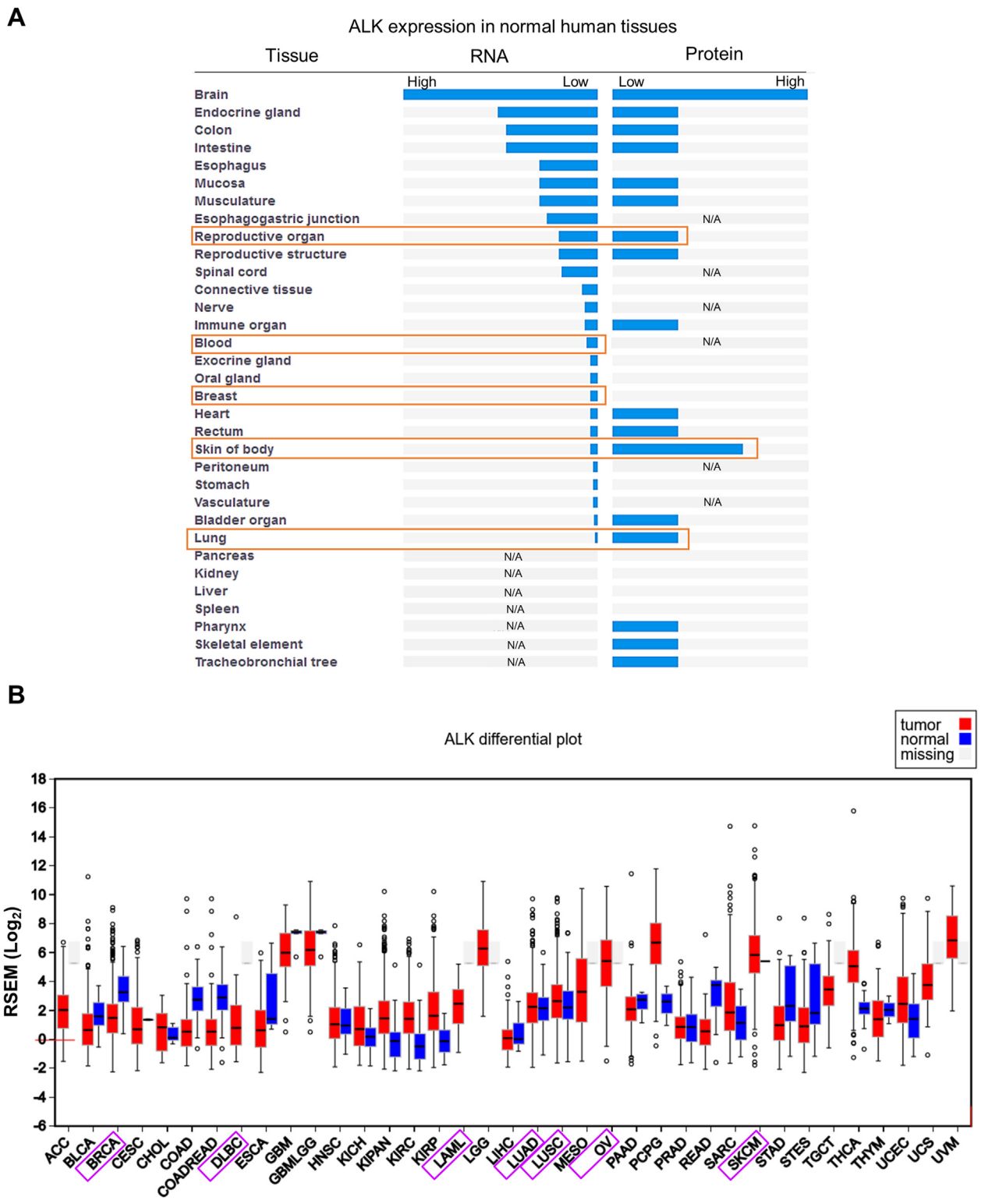

Figure 1. Expression profile of *ALK* across human normal and cancer tissues. **A.** Outline of *ALK* mRNA and protein expression in normal human tissues based on Human Protein Atlas normal tissue immunohistochemistry, Expression Atlas data, and RNA-seq expression data derived from Open Targets Genetics platform. **B.** RSEM (RNA-Seq by Expectation-Maximization) RNA-Seq expression profiles for each cancer and corresponding normal tissue were obtained from The Cancer Genome Atlas (TCGA) using the FireBrowse datasets. The boxes denote the median, and the 25th and 75th % dots symbolize outliers. The red boxes represent tumor tissues and the blue boxes represent corresponding normal tissues. The gray boxes signify that no normal samples exist for that disease cohort. Full form of each cancer type is presented in Table 1.

Table 1. Full form of cancer type used in Figure 1B.

Short-form	Full-form	Cancer/Malignant type
ACC	Adrenocortical carcinoma	Adrenal gland
BLCA	Bladder Urothelial Carcinoma	Bladder
BRCA	Breast invasive carcinoma	Breast
CESC	Cervical squamous cell carcinoma and endocervical adenocarcinoma	Cervical
CHOL	Cholangiocarcinoma	Bile duct
COAD	Colon adenocarcinoma	Colon
COADREAD	Colorectal adenocarcinoma	Colorectal
DLBC	Lymphoid Neoplasm Diffuse Large B-cell Lymphoma	Lymphoma
ESCA	Esophageal carcinoma	Esophageal
GBM	Glioblastoma multiforme	Brain or spinal cord
GBMLGG	Glioma	Brain
HNSC	Head and Neck squamous cell carcinoma	Head and neck
KICH	Kidney Chromophobe	Kidney
KIPAN	Pan-kidney cohort (KICH + KIRC + KIRP)	Kidney
KIRC	Kidney renal clear cell carcinoma	Kidney
KIRP	Kidney renal papillary cell carcinoma	Kidney
LAML	Acute Myeloid Leukemia	Blood
LGG	Brain Lower Grade Glioma	Brain
LIHC	Liver hepatocellular carcinoma	Liver
LUAD	Lung adenocarcinoma	Lung
LUSC	Lung squamous cell carcinoma	Lung
MESO	Mesothelioma	Mesothelium
OV	Ovarian serous cystadenocarcinoma	Ovarian
PAAD	Pancreatic adenocarcinoma	Pancreatic
PCPG	Pheochromocytoma and Paraganglioma	Adrenal medulla/ extra-adrenal ganglia
PRAD	Prostate adenocarcinoma	Prostate
READ	Rectum adenocarcinoma	Rectal
SARC	Sarcoma	Bone/muscle
SKCM	Skin Cutaneous Melanoma	Skin
STAD	Stomach adenocarcinoma	Stomach
STES	Stomach and Esophageal carcinoma	Stomach/esophageal
TGCT	Testicular Germ Cell Tumors	Testis
THCA	Thyroid carcinoma	Thyroid
THYM	Thymoma	Thymus
UCEC	Uterine Corpus Endometrial Carcinoma	Uterus
UCM	Uterine Carcinosarcoma	Uterus
UVM	Uveal Melanoma	Eye

of disease genotypes and phenotypes for human health [17, 18]. One-dimensional omics data for cancer studies provide only limited information regarding the etiology of oncogenesis and cancer progression [19]. In contrast, multi-omics data can provide a greater understanding of the prognosis and predictive precision of disease phenotypes, thereby improving therapeutic and prevention measurements [20]. Prediction of cancer prognosis is an important factor of interest for clinicians, cancer patients, and healthcare professionals as it facilitates all types of decisions concerning patient care and clinical treatment [21]. Therefore, prognostic biomarkers have been employed to precisely select patient subgroups that would benefit from various treatment approaches.

In this study, we comprehensively analyzed *ALK* expression and its clinical significance in lung adenocarcinoma (LUAD), melanoma, ovarian carcinoma (OV), DLBC, AML, and BC patients using publicly available multi-platform datasets. We evaluated gene and mRNA expression patterns, patient prognosis, genetic alteration, protein–protein interaction network, gene co-expression, miRNA co-expression, gene ontology, and signaling pathways in human LUAD, melanoma, OV, DLBC, AML, and BC. The combined data provide supporting evidence for the use of *ALK* as a prognostic biomarker and therapeutic target in *ALK*-positive cancers.

2. Results

2.1. Expression profile of ALK across human normal and cancer tissues

We observed *ALK* RNA and protein expression in various normal human tissues using the Open Target Genetics platform [22]. Both the RNA and protein expression levels of *ALK* were the highest in the brain. *ALK* expression was higher in the skin, reproductive, and lung tissues than in the blood and breast tissues (Figure 1A). The FireBrowse dataset [23] was then used to examine *ALK* transcript expression in multiple human cancers. The results revealed an almost similar pattern of *ALK* gene expression in the corresponding cancer tissues (Figure 1B and Table 1), which primarily suggests that *ALK* is involved in the tumorigenesis of the skin, ovary, lungs, blood, and breast cancers.

2.2. Significant variation in ALK expression in different cancer types

Next, the interactive tool Oncomine [24] was used to assess the mRNA expression of *ALK* in lung, skin, ovary, blood, and breast cancers. As shown in Figure 2, *ALK* mRNA expression was significantly higher in the lung (LUSC and LUAD), skin (CM), and ovary (OSC) and lower in the blood (DLBC and AML) and invasive breast cancer (IBC) than that observed in healthy controls. The results provide strong evidence of the upregulation of *ALK* in LUSC, LUAD, CM, and OSC, and its downregulation in DLBC, AML, and IBC tissues compared to that in their corresponding normal tissues.

2.3. Prognostic investigation of ALK mRNA expression in patients with cancer

The correlation between the level of *ALK* expression and the survival rate of patients with lung, skin, ovarian, blood, and breast cancers was determined using the PrognoScan dataset [25] with significant Cox *p*-values (<0.05). Based on the analysis, *ALK* overexpression was negatively correlated to the survival rate of patients with LUAD (Jacob-00182-UM dataset), melanoma (GSE19234), and ovarian cancers (GSE9891) with increased risk association (hazard ratio [HR] > 1) (Figure 3A–C and I, Table 2). In contrast, the differential expression of *ALK* was associated with a higher death rate in DLBCL (E-TABM-346), AML (GSE8970), and BC (GSE9893) with lower hazard ratios (HR > 0.5) (Figure 3D–F and I). The dataset GSE8894 also revealed that lower expression of *ALK* decreases the survival rate of patients with NSCLC, whereas higher expression leads to lower relapse-free survival with higher risk (HR > 1) in breast cancers, as shown in Figure 3G–H and Table 2. Therefore, our findings suggest that the deregulated expression of *ALK* could lead to poor patient prognosis.

2.4. Evaluation of ALK alteration in associated cancers

Data on genetic alterations in the *ALK* gene and their relevance and expression in different cancers were obtained from the cBioPortal server [26]. Based on the data, 234 alterations were identified from 1–1620 amino acid sequences (Figure 4A and Supplementary Table S1). Of them eight are driver mutations and the remaining mutations are variant of uncertain significance (VUS). The most common type was missense mutations (202 mutations), followed by 17 truncating mutations (including nonsense, frameshift deletion, frameshift insertion, and splicing), 7 gene fusions, 5 splicing, and 3 in-frame mutations. The alteration frequency was the highest in melanoma (15.9% in 444 cases) and the lowest in AML (<1% in 200 cases) (Figure 4B). No gene alterations were found in DLBC. As depicted in Figure 4C, profiling of

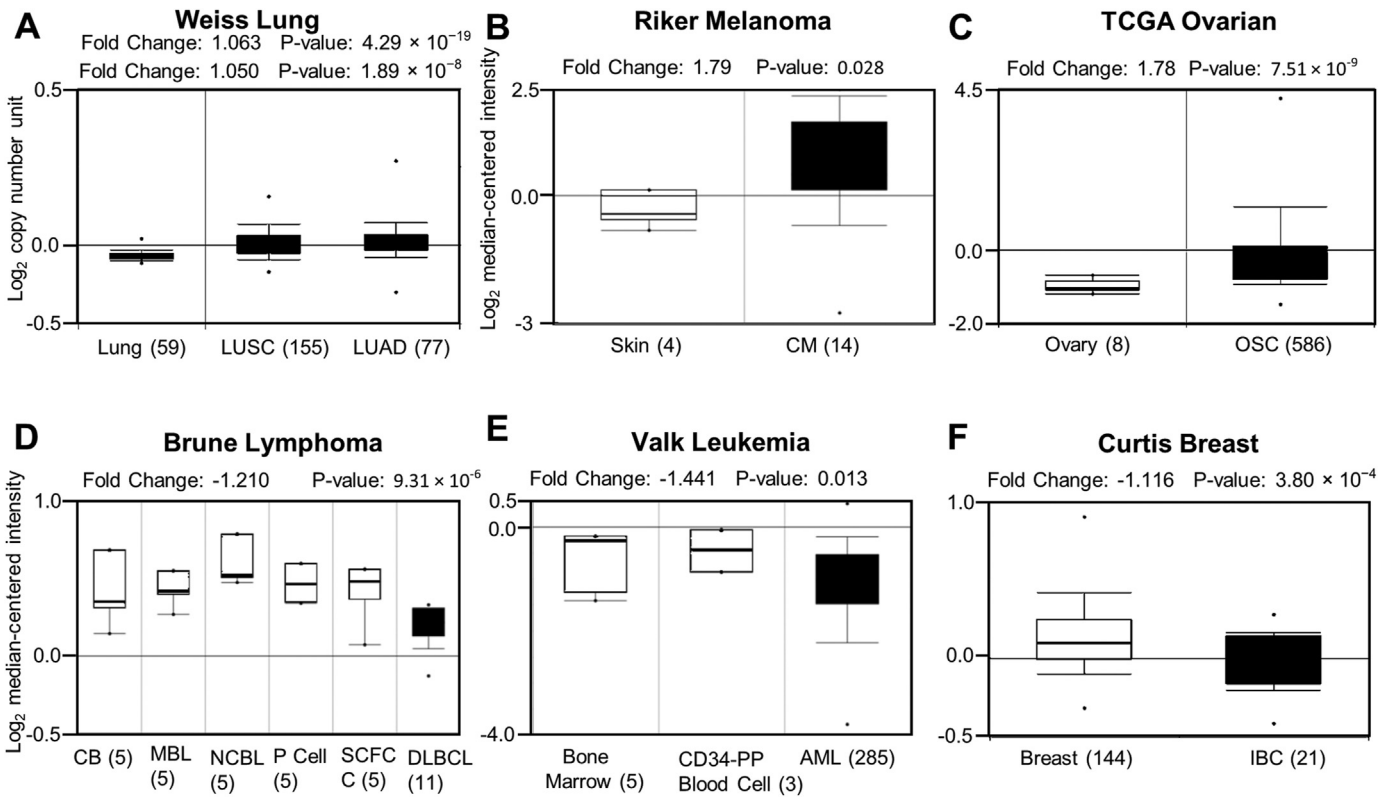

Figure 2. *ALK* expression pattern in various cancer types. **A–F.** *ALK* expression in six cancer types derived from the Oncomine cancer microarray database. The left box plot represents *ALK* expression in normal tissue, while the box on the right represents cancer tissue. Statistically significant differences between normal and cancerous tissues are indicated by $p < 0.05$. LUSC, lung squamous cell carcinoma; LUAD, lung adenocarcinoma; CM, cutaneous melanoma; OSC, ovarian serous carcinoma CB, Centroblast; MBL, Memory B-lymphocyte; NCBL, Naive Pre-germinal Center B-lymphocyte; P cell, Plasma Cell; SCFC, Small Cleaved Follicle Center Cell; DLBCL, diffuse large B-cell lymphoma; CD-34 PP, CD34-Positive Peripheral Blood cell; AML, acute myeloid leukemia; and IBC, invasive breast carcinoma. *ALK* was found to be substantially upregulated in lung, skin, and ovarian cancers, and considerably downregulated in blood and breast cancers. The sample numbers are indicated in parentheses.

mutated RNA expression shows that missense mutations are present in each cancer type (highest in melanoma), seven oncofusions, nine truncating mutations, two splicing mutations, and one in-frame mutation. In contrast, the frequency of copy number gain was the highest, which was distributed in each of the cancers, followed by copy number diploid, shallow deletion, amplification, and deep deletion. Consequently, these results suggest that the overexpression or downregulation of *ALK* in LUAD, skin melanoma, ovarian cancer, AML, DLBC, and BC, respectively, is correlated with mutations and copy number alterations.

2.5. *ALK* protein network analysis and clinical significance in cancers

To understand the significance of the diseases and predict the association between genotype and phenotype, GeneMANIA and STRING servers using Cytoscape_v3.8.2 software were used to construct a protein network. Based on the results, the predicted 20 protein partners from the GeneMANIA server were EPHB3, MDK, AMELY, PTPRB, PTPRZ1, SEC16B, EPHA1, PTPRG, SEC16A, JAK3, MMP13, FBXO24, PTN, ZC3HC1, PDLIM3, MYBPC2, PTPRJ, KRT74, MTIF2, and SHC3 ([1]see footnote for abbreviations) according to physical interactions, co-expression, co-localization, genetic interactions, and shared protein domains (Figure 5A). Ten proteins were identified in the STRING server, including EML4, FRS3, PIK3CA, TNFRSF8, JAK3, PLCG1, KRAS, NPM1, HRAS, and JAK2 ([2]see footnote) (Figure 5B). The genetic alteration frequency of ALK and the 30 interacting protein partners in the six cancer types were subsequently analyzed using cBioPortal. The highest alteration frequency was observed in skin melanoma (70%), followed by LUAD (65%), IBC (58%), and OC (57%), while the lowest was observed in AML (36%) (Figure 5C). These alterations in 17 mutual (Table 3) proteins decreased the patient's disease-free survival compared to the unaltered group in all six cancer types (Figure 5D). Such findings indicate that the identified ALK and its protein partners might be associated with LUAD, SM, OC, DLBC, AML, and BC. Furthermore, genetic alterations in these proteins can affect the clinical outcomes.

[1] EPHB3 (Ephrin type-B receptor 3), MDK (Midkine), AMELY (Amelogenin Y-Linked), PTPRB (Receptor-type tyrosine-protein phosphatase beta), PTPRZ1 (Receptor-type tyrosine-protein phosphatase zeta), SEC16B (SEC16 Homolog B, Endoplasmic Reticulum Export Factor), EPHA1 (Ephrin Type-A Receptor 1), PTPRG (Receptor-Type Tyrosine-Protein Phosphatase Gamma), SEC16A (SEC16 Homolog A, Endoplasmic Reticulum Export Factor), JAK3 (Janus Kinase 3), MMP13 (Matrix Metallopeptidase 13), FBXO24 (F-Box Protein 24), PTN (Pleiotrophin), ZC3HC1 (Zinc Finger C3HC-Type Containing 1), PDLIM3 (PDZ And LIM Domain 3), MYBPC2 (Myosin Binding Protein C2), PTPRJ (Protein Tyrosine Phosphatase Receptor Type J), KRT74 (Keratin 74), MTIF2 (Mitochondrial Translational Initiation Factor 2), and SHC3 (SHC Adaptor Protein 3).

[2] EML4 (Echinoderm Microtubule-Associated Protein-Like 4), FRS3 (Fibroblast Growth Factor Receptor Substrate 3), PIK3CA (Phosphatidylinositol-4,5-Bisphosphate 3-Kinase Catalytic Subunit Alpha), TNFRSF8 (Tumor Necrosis Factor Receptor Superfamily Member 8), JAK3 (Janus Kinase 3), PLCG1 (Phospholipase C Gamma 1), KRAS (Kirsten Rat Sarcoma Viral Oncogene Homolog), NPM1 (Nucleophosmin 1), HRAS (Harvey Rat Sarcoma Viral Oncogene Homolog), and JAK2 (Janus Kinase 2).

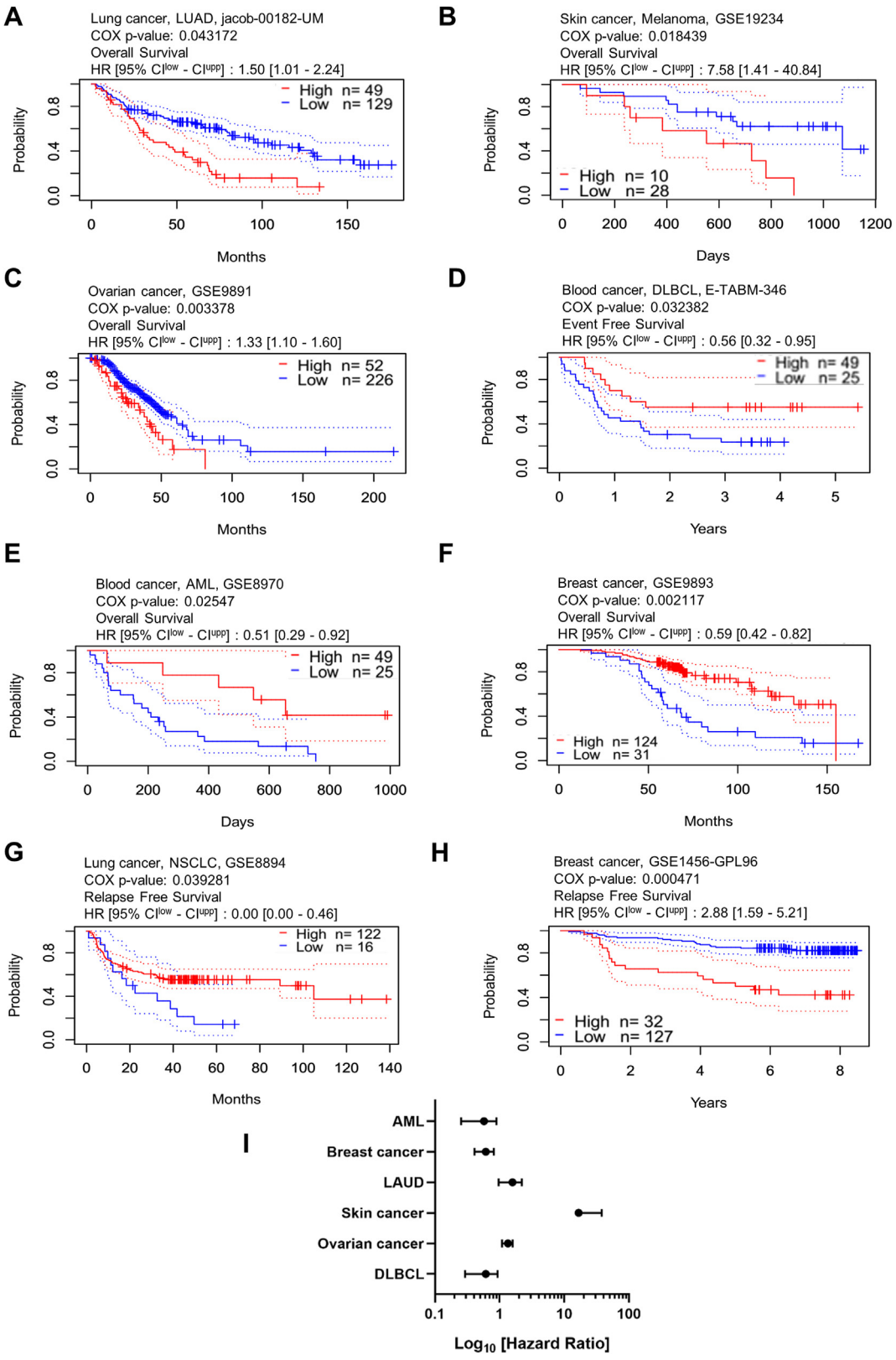

Figure 3. *ALK* expression and clinical prognosis in six different cancers retrieved from PrognoScan microarray cancer database. Kaplan–Meier patient survival estimate of **A.** lung adenocarcinoma, **B.** melanoma, **C.** ovarian cancer, **D–E.** blood cancer: DLBCL and AML, **F.** breast cancer for *ALK* expression, **G.** NSCLC, and **H.** breast cancer for ALK expression. The survival curve was determined as the threshold of the Cox *p*-value < 0.05 and *p*-value < 0.01. The red line denotes high expression and the blue line denotes low expression. The dotted line represents the maximum and minimum values of the average survival. HR, hazard ratio; CI, confidence interval; and n, number of patients. **I.** The statistically significant hazard ratio for the six different cancers was determined from Figure A–F and expressed as a forest plot.

Table 2. Relationship between *ALK* expression and survival in various cancers.

Cancer type	Subtype	Dataset	Endpoint	Array type	Probe id	N	Minimum *p*-value	Cox *p*-value	HR [95% ci^{low} - ci^{upp}]
Lung	NSCLC	GSE8894	Relapse-free survival	HG-U133_Plus_2	208211_s_at	138	0.021281	0.039281	0.00 [0.00–0.46]
	Adenocarcinoma	jacob-00182-UM	Overall survival	HG-U133A	208212_s_at	178	0.000015	0.043172	1.50 [1.01–2.24]
Skin	Melanoma	GSE19234	Overall survival	HG-U133_Plus_2	208211_s_at	38	0.008206	0.018439	7.58 [1.41–40.84]
Ovarian		GSE9891	Overall survival	HG-U133_Plus_2	208212_s_at	278	0.001838	0.003378	1.33 [1.10–1.60]
Brain	Astrocytoma	GSE4271-GPL96	Overall survival	HG-U133A	208211_s_at	77	0.002484	0.080639	1.30 [0.97–1.74]
	Glioblastoma	GSE7696	Overall survival	HG-U133_Plus_2	208212_s_at	70	0.013752	0.133669	0.76 [0.54–1.09]
Breast		GSE1456-GPL96	Relapse-free survival	HG-U133A	208211_s_at	159	0.000001	0.000471	2.88 [1.59–5.21]
		GSE9893	Overall survival	MLRG Human 21K V12.0	5325	155	0.000009	0.002117	0.59 [0.42–0.82]
		GSE1379	Relapse-free survival	Arcturus 22k	4477	60	0.004926	0.022674	1.75 [1.08–2.83]
		GSE6532-GPL570	Relapse-free survival	HG-U133_Plus_2	208211_s_at	87	0.002255	0.032822	5.98 [1.16–30.92]
Colorectal		GSE17536	Disease-free survival	HG-U133_Plus_2	208212_s_at	145	0.012683	0.192777	3.77 [0.35–41.19]
		GSE17537	Overall survival	HG-U133_Plus_2	208212_s_at	55	0.050980	0.19	6.31 [0.40–100.26]
Blood	AML	GSE8970	Overall survival	HG-U133A	208212_s_at	34	0.007686	0.025477	0.51 [0.29–0.92]
	DLBCL	E-TABM-346	Event-free survival	HG-U133A	208211_s_at	53	0.021253	0.032382	0.56 [0.32–0.95]
Prostate		GSE16560	Overall survival	6K DASL	DAP1_1042	281	0.006261	0.112844	1.03 [0.93–1.12]

2.6. Profiling of genes and miRNA co-occurring and co-expressed with ALK

We identified mutually exclusive co-occurrence genes from the 30 ALK protein partners identified using cBioPortal [26]. A total of 17 genes were found to exclusively co-occur with *ALK* based on the *q*-values (<0.05), which are listed in Table 3. *EML4* was identified as the most mutually exclusive gene (odds ratio >3, *q*-value < 0.001) among all genes, whereas *ZC3HC1* had the lowest exclusivity (odds ratio = 1.33, q-value = 0.036). Genetic alterations were also found to be the highest in *EPHB3* (11%).

To assess co-expression, we collected the fold-change values of *ALK* and identified 17 genes from the microarray datasets of the Oncomine server [24]. Expression analysis revealed that all genes were either overexpressed or downregulated in LUAD, CM, OSC, DLBC, AML, and BC, as depicted in the heatmap (Figure 6A). Notably, *MTIF2* and *EPHB3* were overexpressed in these six cancers, whereas *JAK2* and *SHC3* were downregulated in all cancers, except DLBC and AML, respectively. The results indicate that *ALK* and the identified genes were associated with these cancers, either positively or negatively. To determine the impact of each gene expression on the expression of another gene, we used a similarity matrix analysis of the genes with their co-expression values using Morpheus [27]. As shown in Figure 6B, the expression of one gene affected that of another. This finding suggests that the identified co-expressed genes of *ALK* may be associated with the progression of the six cancer types included in our study.

We determined whether the miRNA were co-expressed with *ALK* and 17 common genes using the Enrichr server [28] based on *p*-value ranking (<0.05). Based on the analysis, 19 of the 382 substantially co-expressed miRNAs in humans were identified, as shown in Figure 7 (green node). These findings indicate that the identified miRNAs might contribute to LUAD, SM, OC, DBLC, AML, and BC development, along with *ALK* and common genes.

2.7. Gene ontologies and signaling pathway elucidation of ALK and its correlated genes

Based on the expression profile of *ALK* and its mutual genes, we determined gene ontological features and enrichment pathways using the Enrichr server [28] for integrative analysis of the progression of LUAD, SM, OC, DLBC, AML, and BC in humans. The resulting gene ontology (GO) terms mainly included the transmembrane receptor protein tyrosine kinase signaling pathway, protein autophosphorylation, negative regulation of cell communication (Figure 8A), protein kinase binding, protein tyrosine kinase activity, MAPK activity, growth factor receptor binding (Figure 8B), an integral component of the plasma membrane, specific granule membrane, and endosome lumen activity (Figure 8C). For pathway identification, we considered the results from three datasets, as shown in Figure 8D–F. For the Reactome 2016 datasets, axon guidance, ERK activation, VEGFR2 mediated cell proliferation, and FCERI-mediated MAPK activation were considered (Figure 8D). Analysis of data from PANTHER 2016 revealed the involvement of PDGF signaling, JAK/STAT signaling, angiogenesis, EGFR signaling, chemokine and cytokine signaling, histamine H1 receptor and interferon-gamma signaling, and axon guidance pathways (Figure 8E). Finally, KEGG 2019 suggested pathways related to NSCLC, Th1, Th2, and T17 cell differentiation, pathways in cancer, axon guidance, chemokine and prolactin signaling, adherens junction, glioma, and ErbB signaling (Figure 8F). Therefore, these pathways might be involved in the tumorigenesis of LUAD, SM, OC, DLBC, AML, and BC.

3. Discussion

In this study, by using the Open Targets Genetics portal, we found that *ALK* is highly expressed in lung, skin, and ovary normal tissues compared with that in blood and breast tissues (Figure 1A). Further, by using FireBrowse and Oncomine, we revealed that *ALK* expression at the mRNA and protein levels had similar expression patterns in their respective cancer tissues, such as upregulation in LUAD, melanoma, OC and downregulation in DLBC, AML, and BC (Figure 1B and Figure 2). These findings indicate an association between *ALK* expression and the progression of these six cancers. This finding was consistent with the biological fact that *ALK* expression is upregulated in lung cancer [2, 29, 30], melanoma [31], and OC [6], and downregulated in DLBC [32], AML [33], and BC [9] tissue samples.

Prediction of a disease phenotype based on specific gene expression substantially contributes to patient care with different treatment strategies. Therefore, it is necessary to have a strong prognostic index that facilitates the treatment of LUAD, melanoma, OC, DLBC, AML, and BC. Based on the prognostic analysis results, we found that the overexpression of *ALK* positively correlates with the progression of LUAD,

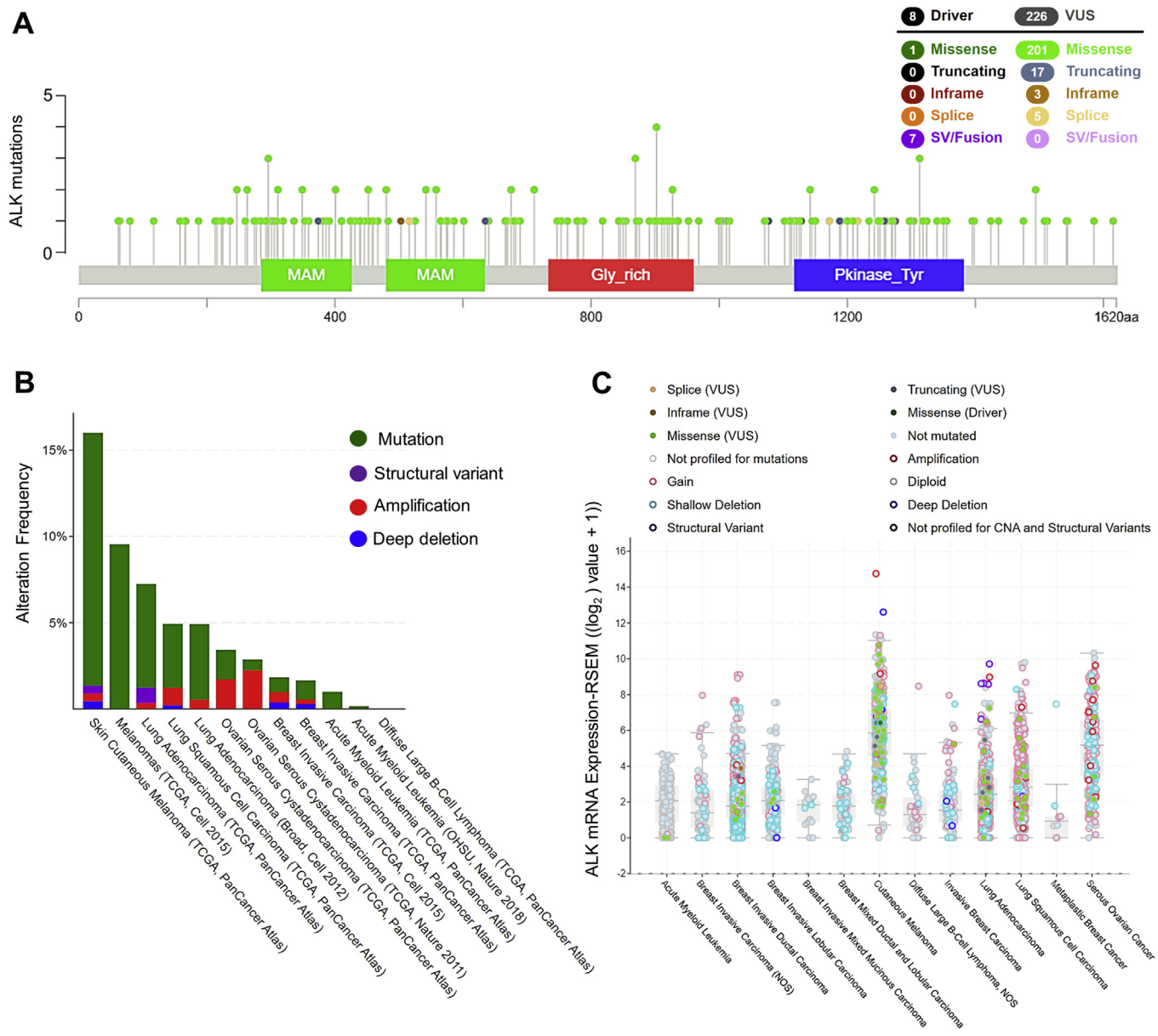

Figure 4. Data on genetic alteration of *ALK* and consequent cancers in patients derived from TCGA PanCancer Atlas database through cBioPortal. **A.** Schematic of the ALK protein and its associated functional domains with the physical location of mutations. A total of 234 alterations were found from 1–1620 amino acid sequences, where 8 are driver and 226 VUS mutations respectively. The highest alteration type was a missense mutation (202) and the lowest was an in-frame mutation (3). **B.** The alteration frequencies of *ALK* and their associated cancers. The Y-axis shows the alteration frequency percentage, and the X-axis represents the type of cancers resulting from the alterations, including mutation and copy number alterations (CAN). The highest alteration frequency was found in melanoma (gene-altered 15.9% in 444 cases). **C.** RNA seq v2 results of genetically altered *ALK* mRNA expression in 12 cancer studies obtained from the cBioPortal web. The mutations included missense mutations in all cancer types (green dots), seven oncofusion in LUAD and melanoma (violet dots), nine truncating (gray dots), three slicing (light brown dots), and one in-frame mutation (deep brown dot). The frequency of copy number gain was the highest and distributed in all cancer types, followed by copy number diploid, shallow deletion, amplification, and deep deletion as indicated in different colors.

melanoma, and OC with higher hazard risk (HR > 1), whereas the downregulation of *ALK* was negatively correlated with the survival rate of patients with DLBC, AML, and BC with relatively lower hazard risk (Figure 3). Previous studies on LUAD and melanoma revealed that *EML4-ALK* rearrangement is associated with a poorer disease-free survival rate than that for *ALK*-negative cancers [34, 35]. However, patients with *ALK* rearrangement have a better prognosis for ovarian cancer than those without *ALK* rearrangement [36]. Our findings are consistent with a previous study on BC showing that patients with ALK protein overexpression exhibited poor overall survival or relapse-free survival compared to those with low ALK expression [37] (Figure 3G–H). These studies, except the study on BC, presented the patient survival rate based on *ALK*-positive or *ALK*-negative samples, whereas our study revealed prognosis based on *ALK* expression levels. To date, no prognostic studies on DLBC and AML based on *ALK* expression patterns have been found. Thus, it is worthwhile to conduct further studies on the overexpression or downregulation of *ALK* for long-term follow-up and a detailed molecular analysis to identify *ALK* as a prognostic biomarker for patients with LUAD, melanoma, OC, DLBC, AML, and BC.

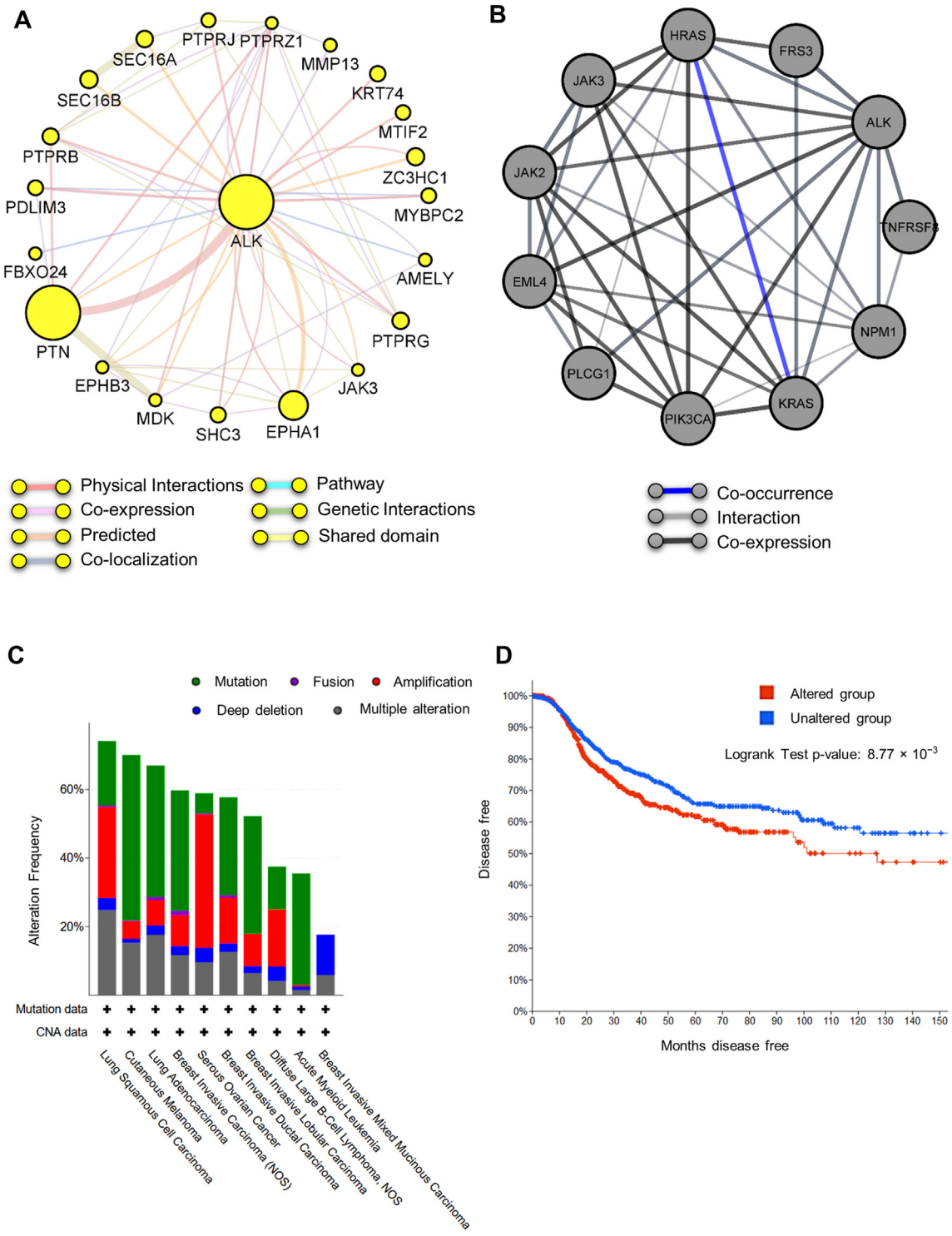

Figure 5. Protein network of ALK and their clinical significance in six cancers. **A–B.** Predicted functional protein partners of ALK generated by considering physical interaction, co-expression, co-localization, genetic interactions, and shared protein domains from GeneMANIA and STRING web servers using Cytoscape_v3.8.2 software. **C.** The genetic alteration frequency of 30 gene signatures in panels A–B was generated for lung, melanoma, ovarian, DLBC, AML, and breast cancers using the cBioPortal platform. The highest alteration percentage was reported in lung cancer, followed by melanoma and breast cancer, while the lowest was in AML. **D.** Kaplan–Meier patient survival estimation of patients with genetically altered and unaltered *ALK* and 17 partner genes (Table 3) in six types of cancers generated from cBioPortal. Patients with altered forms of *ALK* and 17 correlated genes showed significantly less survival than those with unaltered forms.

Table 3. Significant co-occurring protein partners of the *ALK* gene signature were obtained using cBioPortal for cancer genomics.

	Protein partner	Alteration (%)	Log_2 Odds Ratio	*q*-value	Tendency
1	EML4	2.1	>3	<0.001	Co-occurrence
2	KRT74	1.8	2.718	<0.001	
3	SEC16A	3	2.611	<0.001	
4	TNFRSF8	2.5	2.441	<0.001	
5	MTIF2	2.1	2.357	<0.001	
6	PTPRJ	2.6	2.312	<0.001	
7	PTPRB	9	2.185	<0.001	
8	PTPRG	4	2.173	<0.001	
9	PLCG1	2.6	2.111	<0.001	
10	EPHA1	4	1.848	<0.001	
11	JAK2	4	1.812	<0.001	
12	SHC3	1.8	1.722	0.02	
13	FBXO24	3	1.674	0.002	
14	JAK3	4	1.655	0.002	
15	MYBPC2	2.8	1.599	0.008	
16	EPHB3	11	1.413	<0.001	
17	ZC3HC1	2.6	1.336	0.036	

The divergent *ALK* expression in the six cancers might be attributed to the many mutations and copy number alterations which were observed in this study (Figure 4 and Supplementary table S1). Cancer development is a chain of histopathological processes that are influenced by four important factors—somatically acquired genetic, transcriptomic, proteomic, and epigenetic changes [38]. Among our queried patients (N = 5939), *ALK* was altered in 4% of patients (248), with a somatic mutation frequency of 3.4%. Herein, missense, truncating, fusion, and in-frame mutations, splicing, copy number gain, amplification, deep deletion, shallow deletion, and diploid were identified (Figure 4). Several studies have also revealed genetic alterations, including mutations and fusion in *ALK* [2, 4, 39]. In contrast to our findings, Chang *et al.* found three recurrent hotspots (R1275Q/*/L, F1245C/I/L/V, and F1174 L/V) in the tyrosine kinase domain and one (R395 H/C) in the MAM domain in a population-scale cohort of different tumor samples [40]. However, we did not identify any cancer hotspots in the queried TCGA samples.

Protein–protein interactions have been used for the analysis of biological processes, disease progression, and downstream signaling, and have been targeted for drug development [41]. In the present study, we identified 30 proteins (10 from STRING and 20 from GeneMANIA) using Cytoscape software. These 30 protein signatures showed an alteration frequency of up to 65% in melanoma and lung cancers. The *PIK3CA* had the highest alteration frequency (22%), and *HRAS* was the least frequently altered gene (1.8%) (Figure 9). Similarly, Millis *et al.* revealed that *PIK3CA* has a mutational frequency of 13% in solid tumors [42]. In another study, this gene was revealed to be amplified by 33–42% in lung cancer and 15–27% in ovarian cancer [43]. Hobbs *et al.* also reported that HRAS is the least frequent (4%) protein relative to other isoforms, such as KRAS (85%), in human cancers [44]. These results suggest the involvement of PIK3CA, HRAS, and other partners in various cancers.

Using the cBioPortal datasets, we identified 17 genes that exclusively co-occurred with 30 genes (Table 3). Based on our analysis, *EML4* was identified as the most correlated gene. Soda *et al.* (2007) first reported the fusion of *EML4* with *ALK*, an oncogenic driver leading to NSCLC, which was later identified in colorectal cancer and BC [2, 45]. Other genes, such as *EPHB3*, *PTPRJ*, *PTPRB*, and *PLCG1* in lung cancer [46, 47, 48, 49]; *JAK3* in melanoma; *EPHA1* in OC [50]; *TNFRSF8* (*CD30*) in DLBC [51]; and *PLCG1* and *PTPRG* in BC [49, 52], have been reported. However, no relationship was found for 6 of the 17 genes, including *KRT74*, *MTIF2*, *SHC3*, *FBX O 24*, *MYBPC2*, and *ZC3HC1* in the six cancers included in this study. Nonetheless, co-expression with *ALK* was confirmed in our co-expression analysis (Figure 6). *ALK* was found to be upregulated in LUAD, CM, and OSC and downregulated in DLBC, AML, and IBC. This observation is consistent with those of previous studies [31, 32, 33]. Among the identified miRNAs, hsa-miR-1228, hsa-miR-600, and hsa-miR-542-5p were associated with lung cancer [15, 53, 54]; hsa-miR-3158 and hsa-miR-3145 were found in melanoma [55]; and hsa-miR-3619-3p, hsa-miR-4738, and hsa-miR-1298-5p were found in BC [56, 57, 58]. To date, 11 other miRNAs, namely hsa-miR-27a, hsa--miR-6727-5p, hsa-miR-597-5p, hsa-miR-592, hsa-miR-624-5p, hsa--miR-555, hsa-miR-376a-2-5p, hsa-miR-6824-3p, hsa-miR-1255b-2-3p, hsa-miR-3912-5p, and hsa-miR-6854-3p, have not been identified in the queried cancers.

We evaluated the GO enrichment pathways of biological processes, molecular functions, and cellular components for the functional analysis of *ALK* and its correlated genes. Importantly, receptor tyrosine kinase (RTK) signaling activity was the most relevant in all three GO enrichment pathways (Figure 8A–C). RTKs, such as VEGFRs, FGFRs, PDGFRs, and ALK determine the major signaling pathways that are involved in cell proliferation, differentiation, migration, and cell growth, and their dysregulation is a crucial feature of human cancers, such as lung and breast cancers [59, 60]. ALK is activated via dimerization resulting from autophosphorylation and tyrosine activation of the four substrates of ALK, including MAPK, PI3K, PLC γ, and JAK [12]. We also identified similar signaling pathways in the three signaling pathway databases: Reactome, PANTHER, and KEGG (Figure 8D–F). These pathways are not only associated with NSCLC and BC, but also trigger the progression of melanoma, ovarian cancer, DLBC, and AML tumorigenesis [61, 62, 63, 64]. Further studies are required based on gene silencing and overexpression to identify concrete pathways involved in the progression of *ALK*-mediated melanoma, OC, DLBC, and AML.

In summary, this study revealed the possible relationship between *ALK* expression and the prognosis of patients with LUAD, melanoma, OC, DLBC, AML, and BC using publicly available multiplatform bioinformatics datasets. Based on our data, the genotypic expression of *ALK* was substantially correlated with the clinical phenotype in the six cancers. Our study may help clinicians with precision clinical care and researchers in developing cancer therapies for *ALK*-positive cancers. Additional therapies targeting *ALK* in patients with *ALK*-positive melanoma, OC, DLBC, AML, and BC may increase the survival rate. However, further experimental studies are required to confirm whether *ALK* is a prognostic biomarker.

4. Materials and methods

A schematic of this study is depicted in Figure 10.

4.1. Expression profile of ALK across human normal and cancer tissues

ALK mRNA and protein expression data in normal human tissues were obtained from the Human Protein Atlas, normal tissue immunohistochemistry, Expression Atlas data, and RNA-seq expression data using the Open Targets Genetics Portal (https://genetics.opentargets.org) [22]. Gene expression patterns across normal and cancerous tissues were determined using the FireBrowse (http://firebrowse.org/) datasets [23]. The *ALK* query in the FireBrowse database was performed using the default settings.

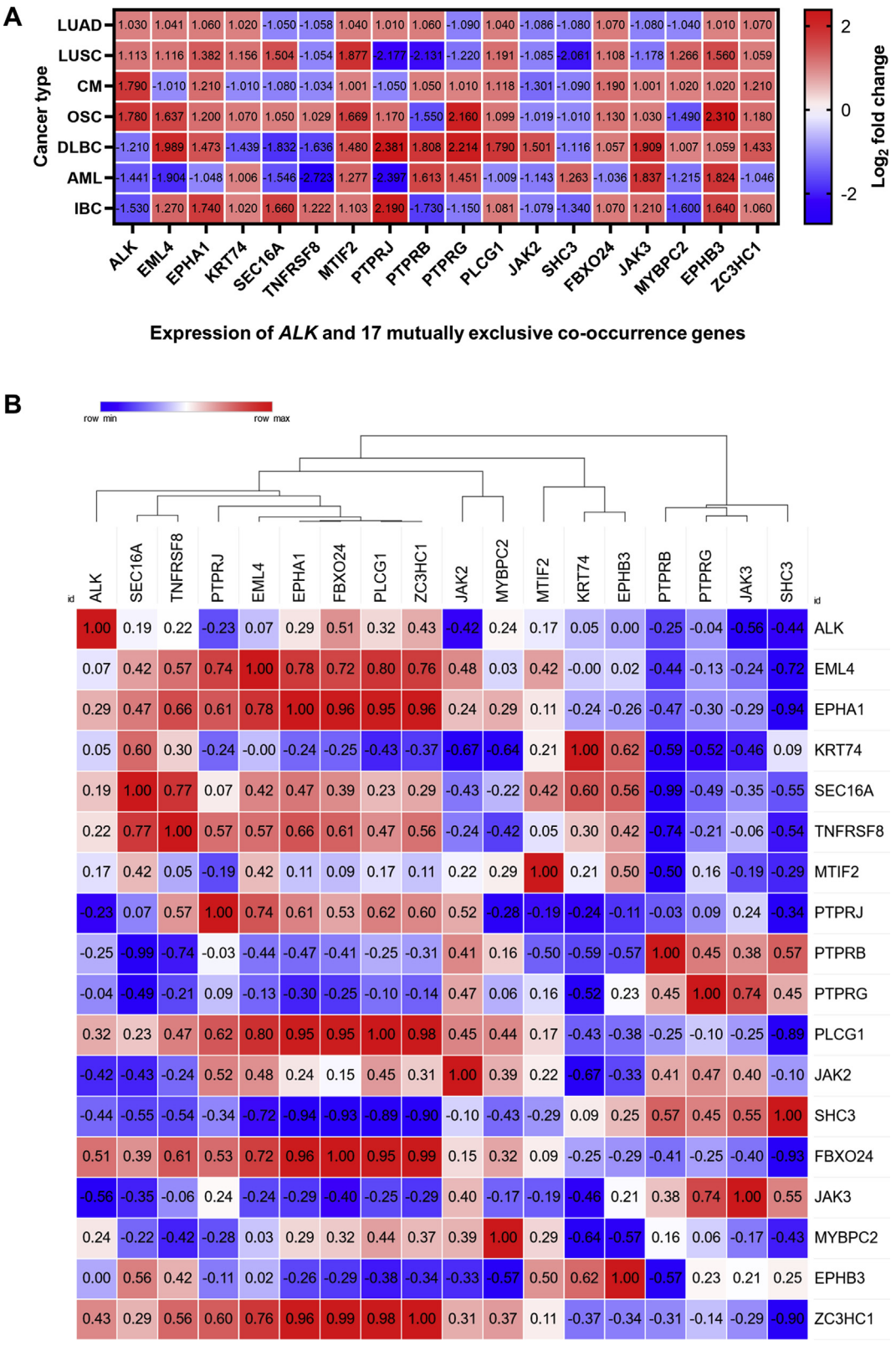

Figure 6. Co-expression and hierarchical clustering analyses. **A.** Co-expression analysis of *ALK* and its 17 mutually associated functional protein partner genes in six cancer types. The heat map was generated from the $\log_2$ fold-change expression value of *ALK* and mutually exclusive protein partner genes retrieved from the cancer microarray database (Oncomine). **B.** Hierarchical clustering and similarity matrix analysis of *ALK* and the expression of correlated genes in six cancer types. The heat map was generated from the $\log_2$ fold-change expression value of *ALK* and common genes retrieved from Oncomine. The outcome of the correlation was visualized using the similarity matrix and hierarchical clustering tools in the Morpheus server.

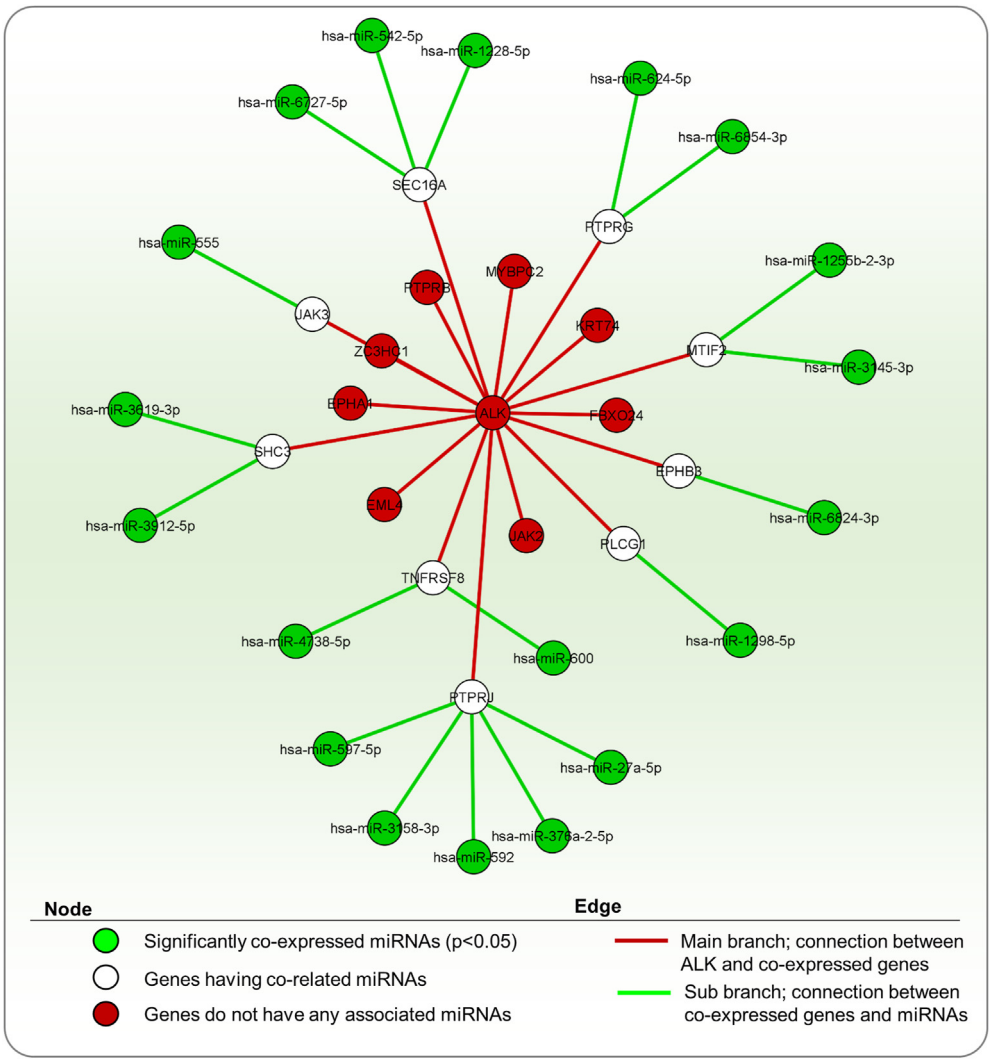

Figure 7. miRNA co-expressed with *ALK* and its mutually exclusive genes in humans. The miRNAs were identified from the Enrichr web portal, and interactions with common genes were analyzed using Cytoscape_v3.8.2 software. The green nodes indicate significantly enriched terms ($p < 0.05$). The white and red nodes denote genes with and without miRNA co-expression, respectively.

4.2. Significant ALK expression variation in different cancer types

The expression levels of the *ALK* gene in lung cancer (LUAD, LUSC), skin cancer (CM), ovarian cancer (OSC), blood cancer (DLBC, AML), and BC and normal tissue counterparts were assessed using the interactive Oncomine (https://www.oncomine.org) dataset [24]. The Oncomine server covers microarray data from 86,733 tumors and 12,764 normal tissues. The following parameters were considered to generate a graph from Oncomine data: *p*-value, <0.05; fold change, 2; gene rank, top 10%.

4.3. Prognostic investigation of ALK mRNA expression in patients with cancer

The biological relationship between *ALK* expression and prognosis of patients with different cancers was assessed using PrognoScan cancer microarray datasets (http://www.prognoscan.org) [25] with a Cox *p*-value of <0.05. PrognoScan provides an effective platform for assessing potential cancer biomarkers and therapeutic targets.

4.4. Evaluation of ALK alteration and associated cancers

TCGA PanCancer Atlas datasets (10,953 patients/10,967 samples) were used to evaluate the genetic alterations of *ALK* in associated cancers, and cBioPortal cancer genomics data (https://www.cbioportal.org) were used to evaluate the RNA-seq-based mRNA expression levels [26].

4.5. ALK protein network analysis and clinical significance in cancers

Protein–protein interaction analysis with the target gene was performed using GeneMANIA and STRING platforms with Cytoscape software version 3.5.2. The predicted 30 proteins were then queried using

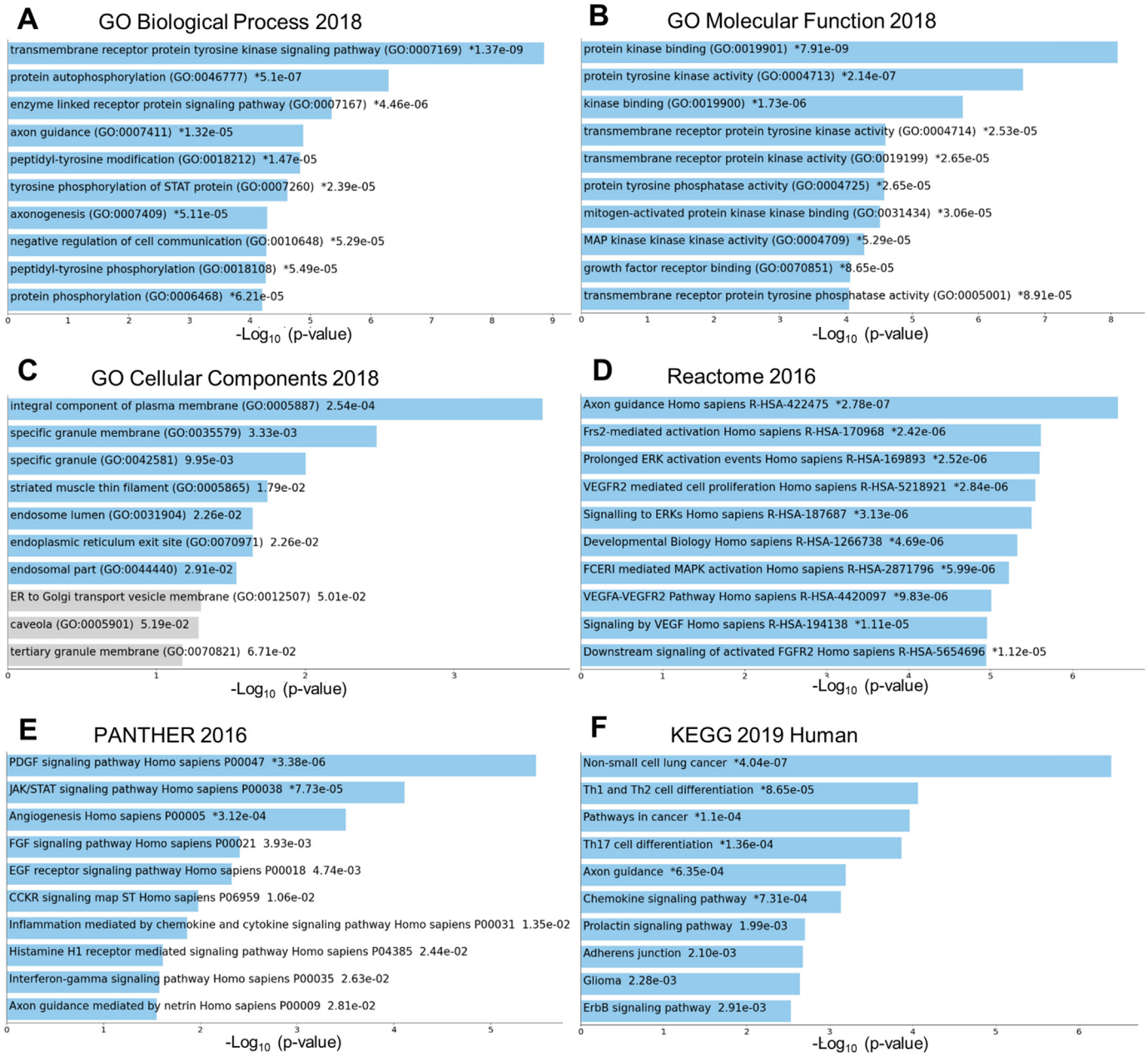

Figure 8. Gene ontology and pathway analyses of ALK and its co-related functional protein partners. **A.** Biological process, **B.** Molecular function, **C.** Cellular components, **D.** Reactome, **E.** PANTHER, and **F.** KEGG pathways of ALK and 18 partner proteins were obtained from the Enrichr web tool. The bar chart shows the top 10 enriched terms in the chosen library, along with their corresponding *p*-values. Colored bars correspond to terms with significant *p*-values (<0.05). * indicates statistically significant values with $p < 0.05$.

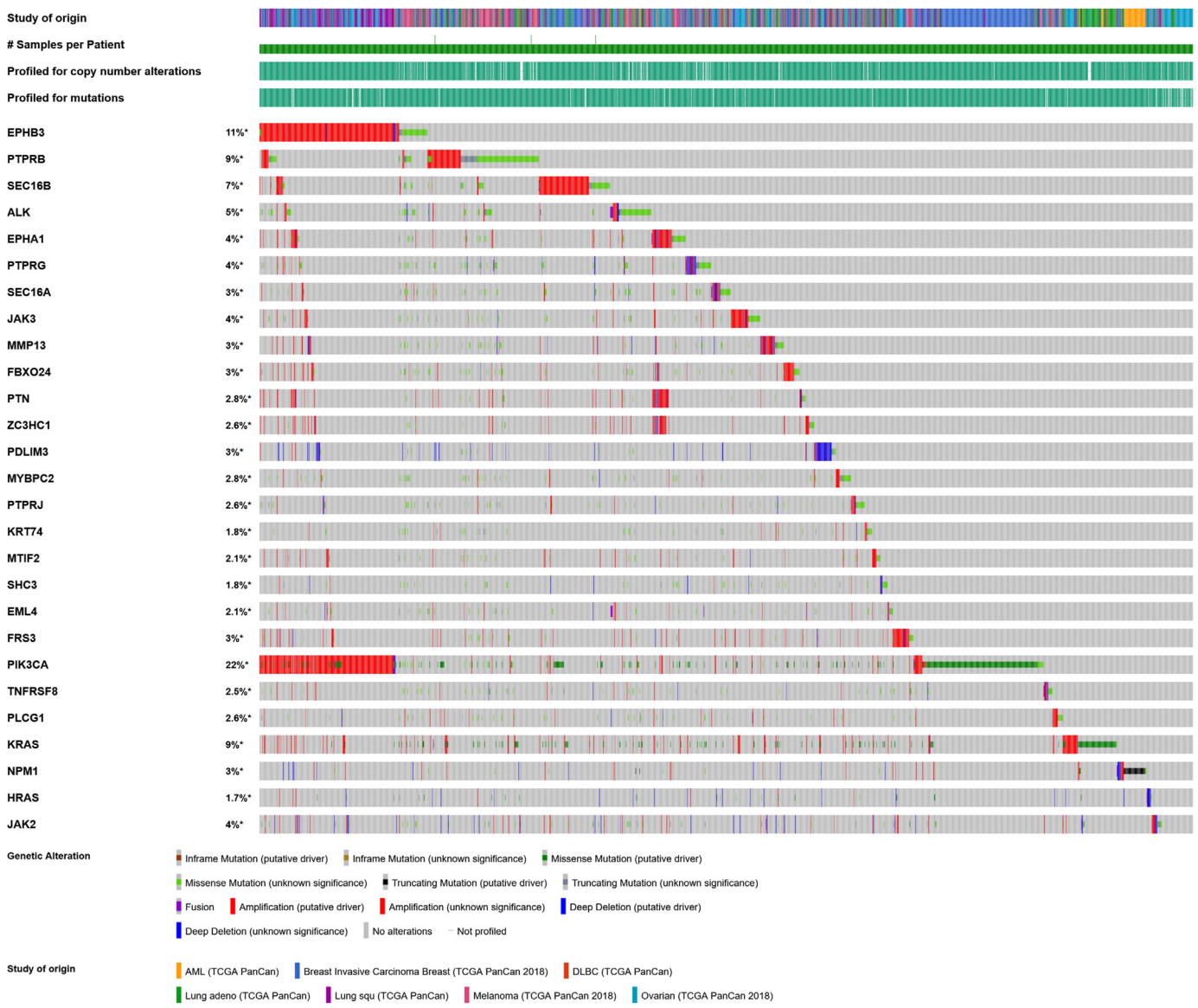

Figure 9. Oncoprint of *ALK* and common genes. The genetic alterations of *ALK* and 17 common genes in six cancers were evaluated using cBioPortal. The highest alteration was observed in *PIK3CA* (22%), followed by *EPHB3* (11%), *KRAS*, and *PTPRB* (9%), while the lowest was observed in *HRAS* (1.7%).

the cBioPortal platform to identify genetic alterations and clinical significance in lung, skin, ovary, blood, and breast cancers.

4.6. Profiling of genes and miRNAs co-occurring and co-expressed with ALK

Genes exclusively co-occurring with the target *ALK* gene were analyzed using the cBioPortal platform based on the *q*-value ranking (<0.05). The co-expression value of the co-occurring genes was obtained using the Oncomine microarray datasets. The co-expression heatmap was generated using GraphPad Prism software version 8 (San Diego, CA, USA). Based on the co-expression values, the influence of one gene on the expression of another gene was evaluated using a similarity matrix and hierarchical clustering tools via the Morpheus server [27]. The miRNAs co-expressed with *ALK* and common genes were obtained from the Enrichr web portal (https://maayanlab.cloud/Enrichr/) [28] and analyzed using Cytoscape_v3.8.2 software.

4.7. Elucidation of gene ontologies and signaling pathways of ALK and its correlated genes

The gene ontologies and signaling pathways of *ALK* with co-occurring genes and relevant bar plots were derived from the Enrichr platform [28]. Enrichr is an integrative web-based gene-list enrichment analysis tool that compares different genomic datasets. The input genes were classified into biological processes, molecular functions, and cellular components according to GO terms. Similarly, signaling pathways were defined using the Reactome 2016, PANTHER 2016, and KEGG 2019. A Cox *p*-value of <0.05 was considered statistically significant for both GO and signaling pathway bar plots.

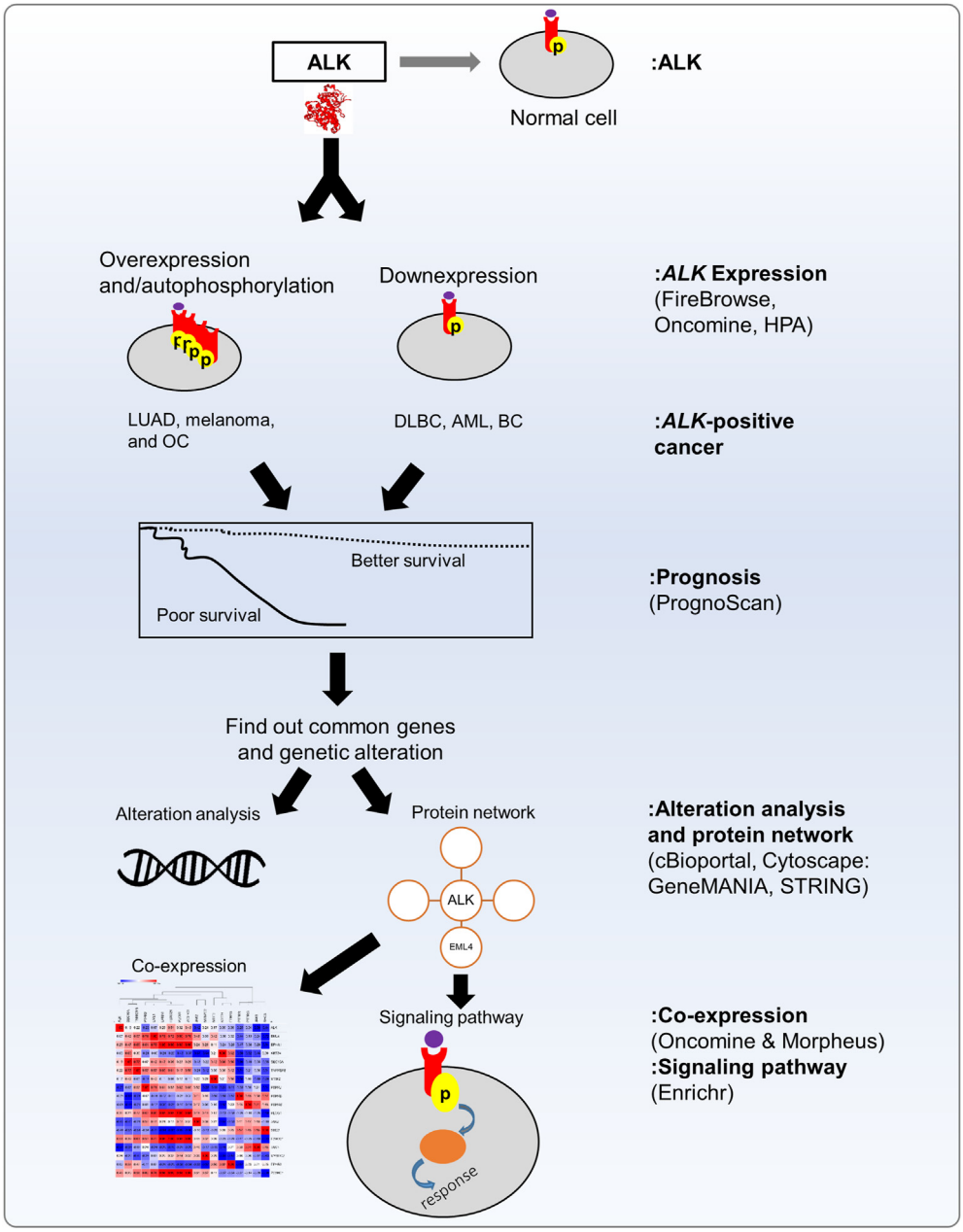

Figure 10. Schematic diagram of this study.

5. Conclusion

In this study, to determine *ALK* as a potential prognostic biomarker in *ALK*-positive LUAD, melanoma, OC, DLBC, AML, and BC progression, we assessed *ALK* expression, genetic mutations, protein–protein interaction networks, correlated genes, and miRNAs, and prognostic values using various publicly available bioinformatics datasets. We conclude that both the upregulation of *ALK* in LUAD, melanoma, and OV, or downregulation in DLBC, AML, and BC progression negatively correlated with patient survival. Furthermore, we revealed the possible gene ontology and signaling pathways associated with *ALK* and its expression in the progression of these six cancers. These pathways may serve as potential targets for inhibiting the development of cancer. Collectively these findings suggest that *ALK* could be an effective prognostic biomarker and a potential therapeutic target to control *ALK*-positive cancers. Further studies using *in vitro* experiments are required to validate our results.

Declarations

Author contribution statement

Saifullah: Conceived and designed the experiments; Performed the experiments; Analyzed and interpreted the data; Wrote the paper.

Toshifumi Tsukahara: Conceived and designed the experiments; Contributed reagents, materials, analysis tools or data; Wrote the paper.

Funding statement

Dr. Toshifumi Tsukahara was supported by the Grant-in-Aid for Scientific Research from the Japan Society for the Promotion of Science [21H02067 and 18K19288].

Saifullah was supported by the scholarship from the Ministry of Education, Culture, Sports, Science, and Technology (MEXT), Japan.

Data availability statement

Data included in article/supp. material/referenced in article.

Declaration of interests statement

The authors declare no competing interests.

Additional information

Supplementary content related to this article has been published online at https://doi.org/10.1016/j.heliyon.2022.e09878.

References

[1] B. Golding, A. Luu, R. Jones, A.M. Viloria-Petit, The function and therapeutic targeting of anaplastic lymphoma kinase (ALK) in non-small cell lung cancer (NSCLC), Mol. Cancer 17 (2018) 52.

[2] M. Soda, Y.L. Choi, M. Enomoto, S. Takada, Y. Yamashita, S. Ishikawa, S.-i. Fujiwara, H. Watanabe, K. Kurashina, H. Hatanaka, et al., Identification of the transforming EML4–ALK fusion gene in non-small-cell lung cancer, Nature 448 (2007) 561–566.

[3] Saifullah, T. Tsukahara, Integrated analysis of ALK higher expression in human cancer and downregulation in LUAD using RNA molecular scissors, Clin. Transl. Oncol. (2022).

[4] S. Morris, M. Kirstein, M. Valentine, K. Dittmer, D. Shapiro, D. Saltman, A. Look, Fusion of a kinase gene, ALK, to a nucleolar protein gene, NPM, in non-Hodgkin's lymphoma, Science 263 (1994) 1281–1284.

[5] G. Cesi, D. Philippidou, I. Kozar, Y.J. Kim, F. Bernardin, G. Van Niel, A. Wienecke-Baldacchino, P. Felten, E. Letellier, S. Dengler, et al., A new ALK isoform transported by extracellular vesicles confers drug resistance to melanoma cells, Mol. Cancer 17 (2018) 145.

[6] H. Ren, Z.-P. Tan, X. Zhu, K. Crosby, H. Haack, J.-M. Ren, S. Beausoleil, A. Moritz, G. Innocenti, J. Rush, et al., Identification of anaplastic lymphoma kinase as a potential therapeutic target in ovarian cancer, Cancer Res. 72 (2012) 3312–3323.

[7] E.A. Morgan, A.F. Nascimento, Anaplastic lymphoma kinase-positive large B-cell lymphoma: an underrecognized aggressive lymphoma, Adv. Hematol. 2012 (2012), 529572.

[8] J.E. Maxson, M.A. Davare, S.B. Luty, C.A. Eide, B.H. Chang, M.M. Loriaux, C.E. Tognon, D. Bottomly, B. Wilmot, S.K. McWeeney, et al., Therapeutically targetable ALK mutations in leukemia, Cancer Res. 75 (2015) 2146–2150.

[9] M.G. Hanna, V. Najfeld, H.Y. Irie, J. Tripodi, A. Nayak, Analysis of ALK gene in 133 patients with breast cancer revealed polysomy of chromosome 2 and no ALK amplification, SpringerPlus 4 (2015) 439.

[10] M. Jeanneau, V. Gregoire, C. Desplechain, F. Escande, D.P. Tica, S. Aubert, X. Leroy, ALK rearrangements-associated renal cell carcinoma (RCC) with unique pathological features in an adult, Pathol. Res. Pract. 212 (2016) 1064–1066.

[11] A. Aubry, S. Galiacy, M. Allouche, Targeting ALK in cancer: therapeutic potential of proapoptotic peptides, Cancers 11 (2019) 275.

[12] C.M. Della Corte, G. Viscardi, R. Di Liello, M. Fasano, E. Martinelli, T. Troiani, F. Ciardiello, F. Morgillo, Role and targeting of anaplastic lymphoma kinase in cancer, Mol. Cancer 17 (2018) 30.

[13] B. Hallberg, R.H. Palmer, The role of the ALK receptor in cancer biology, Ann. Oncol. 27 (2016) iii4-iii15.

[14] T. Matsumoto, Y. Oda, Y. Hasegawa, M. Hashimura, Y. Oguri, H. Inoue, A. Yokoi, M. Tochimoto, M. Nakagawa, Z. Jiang, et al., Anaplastic lymphoma kinase overexpression is associated with aggressive phenotypic characteristics of ovarian high-grade serous carcinoma, Am. J. Pathol. 191 (2021) 1837–1850.

[15] Y. Chen, J. Takita, Y.L. Choi, M. Kato, M. Ohira, M. Sanada, L. Wang, M. Soda, A. Kikuchi, T. Igarashi, et al., Oncogenic mutations of ALK kinase in neuroblastoma, Nature 455 (2008) 971–974.

[16] J. Okubo, J. Takita, Y. Chen, K. Oki, R. Nishimura, M. Kato, M. Sanada, M. Hiwatari, Y. Hayashi, T. Igarashi, et al., Aberrant activation of ALK kinase by a novel truncated form ALK protein in neuroblastoma, Oncogene 31 (2012) 4667–4676.

[17] A. Samad, F. Haque, Z. Nain, R. Alam, M.A. Al Noman, M.H. Rahman Molla, M.S. Hossen, M.R. Islam, M.I. Khan, F. Ahammad, Computational assessment of MCM2 transcriptional expression and identification of the prognostic biomarker for human breast cancer, Heliyon 6 (2020), e05087.

[18] D. Sayeeram, T.V. Katte, S. Bhatia, A. Jai Kumar, A. Kumar, G. Jayashree, D.S. Rachana, H.V. Nalla Reddy, A. Arvind Rasalkar, R.L. Malempati, et al., Identification of potential biomarkers for lung adenocarcinoma, Heliyon 6 (2020).

[19] I. Subramanian, S. Verma, S. Kumar, A. Jere, K. Anamika, Multi-omics data integration, interpretation, and its application, Bioinf. Biol. Insights 14 (2020).

[20] Y. Hasin, M. Seldin, A. Lusis, Multi-omics approaches to disease, Genome Biol. 18 (2017) 83.

[21] B.A. Rabin, B. Gaglio, T. Sanders, L. Nekhlyudov, J.W. Dearing, S. Bull, R.E. Glasgow, A. Marcus, Predicting cancer prognosis using interactive online tools: a systematic review and implications for cancer care providers, Cancer Epidemiol. Biomark. Prev. 22 (2013) 1645–1656.

[22] M. Ghoussaini, E. Mountjoy, M. Carmona, G. Peat, E.M. Schmidt, A. Hercules, L. Fumis, A. Miranda, D. Carvalho-Silva, A. Buniello, et al., Open Targets Genetics: systematic identification of trait-associated genes using large-scale genetics and functional genomics, Nucleic Acids Res. 49 (2021) D1311–d1320.

[23] FireBrowse. Broad Institute, TCGA Genome data analysis center, in: Firehose Stddata_2016_01_28 Run 2016, Broad Institute of MIT and Harvard, 2016, pp. 2498–2504.

[24] D.R. Rhodes, S. Kalyana-Sundaram, V. Mahavisno, R. Varambally, J. Yu, B.B. Briggs, T.R. Barrette, M.J. Anstet, C. Kincead-Beal, P. Kulkarni, et al., Oncomine 3.0: genes, pathways, and networks in a collection of 18,000 cancer gene expression profiles, Neoplasia 9 (2007) 166–180.

[25] H. Mizuno, K. Kitada, K. Nakai, A. Sarai, PrognoScan: a new database for meta-analysis of the prognostic value of genes, BMC Med. Genom. 2 (2009) 18.

[26] J. Gao, B.A. Aksoy, U. Dogrusoz, G. Dresdner, B. Gross, S.O. Sumer, Y. Sun, A. Jacobsen, R. Sinha, E. Larsson, et al., Integrative analysis of complex cancer genomics and clinical profiles using the cBioPortal, Sci. Signal. 6 (2013) pl1, pl1.

[27] Morpheus. https://software.broadinstitute.org/morpheus.

[28] M.V. Kuleshov, M.R. Jones, A.D. Rouillard, N.F. Fernandez, Q. Duan, Z. Wang, S. Koplev, S.L. Jenkins, K.M. Jagodnik, A. Lachmann, et al., Enrichr: a comprehensive gene set enrichment analysis web server 2016 update, Nucleic Acids Res. 44 (2016) W90–W97.

[29] Saifullah, M. Sakari, T. Suzuki, S. Yano, T. Tsukahara, Effective RNA knockdown using CRISPR-cas13a and molecular targeting of the EML4-ALK transcript in H3122 lung cancer cells, Int. J. Mol. Sci. 21 (2020) 8904.

[30] S. Saifullah, M. Sakari, T. Suzuki, S. Yano, T. Tsukahara, P28-11 the CRISPR-Cas13a gene-editing system underlies a potential therapeutic strategy for EML4-ALK-positive lung cancer cells, Ann. Oncol. 32 (2021) S347.

[31] K.J. Busam, R.E. Vilain, T. Lum, J.A. Busam, T.J. Hollmann, R.P.M. Saw, D.C. Coit, R.A. Scolyer, T. Wiesner, Primary and metastatic cutaneous melanomas express ALK through alternative transcriptional initiation, Am. J. Surg. Pathol. 40 (2016) 786–795.

[32] V. Brune, E. Tiacci, I. Pfeil, C. Doring, S. Eckerle, C.J.M. van Noesel, W. Klapper, B. Falini, A. von Heydebreck, D. Metzler, et al., Origin and pathogenesis of nodular lymphocyte–predominant Hodgkin lymphoma as revealed by global gene expression analysis, J. Exp. Med. 205 (2008) 2251–2268.

[33] P.J.M. Valk, R.G.W. Verhaak, M.A. Beijen, C.A.J. Erpelinck, S.B.v.W. van Doorn-Khosrovani, J.M. Boer, H.B. Beverloo, M.J. Moorhouse, P.J. van der Spek, B. Löwenberg, et al., Prognostically useful gene-expression profiles in acute myeloid leukemia, N. Engl. J. Med. 350 (2004) 1617–1628.

[34] J. Shi, W. Gu, Y. Zhao, J. Zhu, G. Jiang, M. Bao, J. Shi, Clinicopathological and prognostic significance of EML4-ALK rearrangement in patients with surgically resected lung adenocarcinoma: a propensity score matching study, Cancer Manag. Res. 12 (2020) 589–598.

[35] S. Cao, V.E. Nambudiri, Anaplastic lymphoma kinase in cutaneous malignancies, Cancers 9 (2017) 123.

[36] R. Bi, Q. Bai, X. Zhu, X. Tu, X. Cai, W. Jiang, X. Xu, S. Tang, H. Ge, B. Chang, et al., ALK rearrangement: a high-frequency alteration in ovarian metastasis from lung adenocarcinoma, Diagn. Pathol. 14 (2019) 96.

[37] A.K. Siraj, S. Beg, Z. Jehan, S. Prabhakaran, M. Ahmed, R. Hussain, F. Al-Dayel, A. Tulbah, D. Ajarim, K.S. Al-Kuraya, ALK alteration is a frequent event in aggressive breast cancers, Breast Cancer Res. 17 (2015) 127.

[38] H. Okayama, T. Kohno, Y. Ishii, Y. Shimada, K. Shiraishi, R. Iwakawa, K. Furuta, K. Tsuta, T. Shibata, S. Yamamoto, et al., Identification of genes upregulated in ALK-Positive and EGFR/KRAS/ALK-Negative lung adenocarcinomas, Cancer Res. 72 (2012) 100–111.

[39] H. Mizuta, K. Okada, M. Araki, J. Adachi, A. Takemoto, J. Kutkowska, K. Maruyama, N. Yanagitani, T. Oh-hara, K. Watanabe, et al., Gilteritinib overcomes lorlatinib resistance in ALK-rearranged cancer, Nat. Commun. 12 (2021) 1261.

[40] M.T. Chang, S. Asthana, S.P. Gao, B.H. Lee, J.S. Chapman, C. Kandoth, J. Gao, N.D. Socci, D.B. Solit, A.B. Olshen, et al., Identifying recurrent mutations in cancer reveals widespread lineage diversity and mutational specificity, Nat. Biotechnol. 34 (2016) 155–163.

[41] L. Laraia, G. McKenzie, David R. Spring, Ashok R. Venkitaraman, David J. Huggins, Overcoming chemical, biological, and computational challenges in the development of inhibitors targeting protein-protein interactions, Chem. Biol. 22 (2015) 689–703.

[42] S.Z. Millis, D.L. Jardim, L. Albacker, J.S. Ross, V.A. Miller, S.M. Ali, R. Kurzrock, Phosphatidylinositol 3-kinase pathway genomic alterations in 60,991 diverse solid tumors informs targeted therapy opportunities, Cancer 125 (2019) 1185–1199.

[43] R. Arafeh, Y. Samuels, PIK3CA in cancer: the past 30 years, Semin. Cancer Biol. 59 (2019) 36–49.

[44] G.A. Hobbs, C.J. Der, K.L. Rossman, RAS isoforms and mutations in cancer at a glance, J. Cell Sci. 129 (2016) 1287–1292.

[45] E. Lin, L. Li, Y. Guan, R. Soriano, C.S. Rivers, S. Mohan, A. Pandita, J. Tang, Z. Modrusan, Exon array profiling detects EML4-ALK fusion in breast, colorectal, and non–small cell lung cancers, Mol. Cancer Res. 7 (2009) 1466–1476.

[46] G. Li, X.-D. Ji, H. Gao, J.-S. Zhao, J.-F. Xu, Z.-J. Sun, Y.-Z. Deng, S. Shi, Y.-X. Feng, Y.-Q. Zhu, et al., EphB3 suppresses non-small-cell lung cancer metastasis via a PP2A/RACK1/Akt signalling complex, Nat. Commun. 3 (2012) 667.

[47] S. D'Agostino, D. Lanzillotta, M. Varano, C. Botta, A. Baldrini, A. Bilotta, S. Scalise, V. Dattilo, R. Amato, E. Gaudio, et al., The receptor protein tyrosine phosphatase PTPRJ negatively modulates the CD98hc oncoprotein in lung cancer cells, Oncotarget 9 (2018).

[48] Y. Qi, Y. Dai, S. Gui, Protein tyrosine phosphatase PTPRB regulates Src phosphorylation and tumour progression in NSCLC, Clin. Exp. Pharmacol. Physiol. 43 (2016) 1004–1012.

[49] H.-J. Jang, P.-G. Suh, Y.J. Lee, K.J. Shin, L. Cocco, Y.C. Chae, PLCγ1: potential arbitrator of cancer progression, Adv. Biol. Regul. 67 (2018) 179–189.

[50] Y. Cui, B. Wu, V. Flamini, B.A.J. Evans, D. Zhou, W.G. Jiang, Knockdown of EPHA1 using CRISPR/CAS9 suppresses aggressive properties of ovarian cancer cells, Anticancer Res. 37 (2017) 4415–4424.

[51] M.Q. Salas, F. Climent, G. Tapia, E. DomingoDomènech, S. Mercadal, A.C. Oliveira, C. Aguilera, G. Olga, M. Moreno Velázquez, M. Andrade-Campos, et al., Clinicopathologic features and prognostic significance of CD30 expression in de novo diffuse large B-cell lymphoma (DLBCL): results in a homogeneous series from a single institution, Biomarkers 25 (2020) 69–75.
[52] Y. Du, J.R. Grandis, Receptor-type protein tyrosine phosphatases in cancer, Chin. J. Cancer 34 (2015) 61–69.
[53] G. Umapathy, P. Mendoza-Garcia, B. Hallberg, R.H. Palmer, Targeting anaplastic lymphoma kinase in neuroblastoma, APMIS 127 (2019) 288–302.
[54] Y. Chi, Q. Luo, Y. Song, F. Yang, Y. Wang, M. Jin, D. Zhang, Circular RNA circPIP5K1A promotes non-small cell lung cancer proliferation and metastasis through miR-600/HIF-1α regulation, J. Cell. Biochem. 120 (2019) 19019–19030.
[55] M.S. Stark, S. Tyagi, D.J. Nancarrow, G.M. Boyle, A.L. Cook, D.C. Whiteman, P.G. Parsons, C. Schmidt, R.A. Sturm, N.K. Hayward, Characterization of the melanoma miRNAome by deep sequencing, PLoS One 5 (2010) e9685.
[56] W. Lou, J. Liu, B. Ding, L. Xu, W. Fan, Identification of chemoresistance-associated miRNAs in breast cancer, Cancer Manag. Res. 10 (2018) 4747–4757.
[57] H. Persson, A. Kvist, N. Rego, J. Staaf, J. Vallon-Christersson, L. Luts, N. Loman, G. Jonsson, H. Naya, M. Hoglund, et al., Identification of new MicroRNAs in paired normal and tumor breast tissue suggests a dual role for the ERBB2/her2 gene, Cancer Res. 71 (2011) 78–86.
[58] J. Zhang, D. Hu, miR-1298-5p Influences the Malignancy Phenotypes of Breast Cancer Cells by Inhibiting CXCL11 13, 2021, pp. 133–145.
[59] M.A. Lemmon, J. Schlessinger, Cell signaling by receptor tyrosine kinases, Cell 141 (2010) 1117–1134.
[60] R. Katayama, C.M. Lovly, A.T. Shaw, Therapeutic targeting of anaplastic lymphoma kinase in lung cancer: a paradigm for precision cancer medicine, Clin. Cancer Res. 21 (2015) 2227–2235.
[61] G.S. Inamdar, S.V. Madhunapantula, G.P. Robertson, Targeting the MAPK pathway in melanoma: why some approaches succeed and other fail, Biochem. Pharmacol. 80 (2010) 624–637.
[62] G. Gritsina, F. Xiao, S.W. O'Brien, R. Gabbasov, M.A. Maglaty, R.-H. Xu, R.J. Thapa, Y. Zhou, E. Nicolas, S. Litwin, et al., Targeted blockade of JAK/STAT3 signaling inhibits ovarian carcinoma growth, Mol. Cancer Therapeut. 14 (2015) 1035–1047.
[63] J.M. Matthews, S. Bhatt, M.P. Patricelli, T.K. Nomanbhoy, X. Jiang, Y. Natkunam, A.J. Gentles, E. Martinez, D. Zhu, J.R. Chapman, et al., Pathophysiological significance and therapeutic targeting of germinal center kinase in diffuse large B-cell lymphoma, Blood 128 (2016) 239–248.
[64] M. Milella, S.M. Kornblau, Z. Estrov, B.Z. Carter, H. Lapillonne, D. Harris, M. Konopleva, S. Zhao, E. Estey, M. Andreeff, Therapeutic targeting of the MEK/MAPK signal transduction module in acute myeloid leukemia, J. Clin. Invest. 108 (2001) 851–859.